



COB-2021-XXXX

CALCULATION OF ISENTROPIC EFFICIENCY AS A FUNCTION OF THE GEOMETRY OF TURBINES OPERATING WITH SUPERCRITICAL CO₂

Matheus Philippe Martins da Cruz

Rafael Augusto Magalhães Ferreira

Universidade Federal de Minas Gerais
matheuspmc@ufmg.br; rafael.ferreira@demec.ufmg.br

Matheus Pereira Porto

Universidade Federal de Minas Gerais
matheusporto@ufmg.br

Abstract. *This paper presents a novel method to estimate turbines performance operating with supercritical CO₂. Current methodologies consider only the inlet and exit rotor angles into the performance estimations, neglecting the geometric characteristics. Also, the current relations are based on the ideal gas model. We used real gas models to assess the supercritical CO₂ performance behavior when the geometry of the blades are changed, even though the rotor inlet and exit cross-sections do not change. As a result, we found that the turbine power varies significantly with the blade geometry due to the pressure-drop losses, during the fluid flow. We compared the real gas and ideal gas models for supercritical CO₂ in the same turbine, and we found that the ideal gas relations underestimates the turbine power output.*

Keywords: *pseudopolytropic expansion, turbine sizing, supercritical CO₂, real gases, turbomachinery.*

1. INTRODUCTION

Supercritical CO₂ Brayton cycles possess higher theoretical efficiency than conventional Brayton cycles (QI et. al., 2017) due to the high density, low viscosity, and high specific heat of the fluid. However, this high efficiency was not achieved in practical applications due to weak mathematical formulations (ideal gas model cannot be applied to s-CO₂, PERSKY AND SAURET, 2019).

Mathematical models used to simulate turbine performance need robust iterative calculations. To do so, they assume a value of efficiency that is considered reasonable and, from there, calculate the other variables of the system (LEE AND GURGENCI). However, many studies use more straightforward, oversimplified methodologies that purposefully avoid iterative computation.

Some studies have already been conducted to improve the s-CO₂ compression and expansion cycle performance, such as Lee and Gurgenci (2020), who discussed the most suitable methodology for a mathematical model for turbine sizing. According to them, the efficiency of a turbine must be carefully calculated, and therefore should be treated as a function of all system variables. They, therefore, used an iterative calculation in their model. Baltadjiev, Claudio, and Spakovsky (2020), meanwhile, questioned an essential factor in the current calculation methodology. The authors noted that the head loss relations available in the literature were formulated considering the thermodynamic relations of ideal gases and that few studies prove the veracity of these models for real gases, such as s-CO₂. Despite this, the use of these relations for carbon dioxide gas is widespread. Finally, despite a large number of studies on supercritical carbon dioxide, the literature still lacks papers that treat the transformations of s-CO₂ as a pseudo-polytropic process. This requires that the polytropic coefficient of the fluid be calculated repeatedly, which is currently possible, thanks to computational resources.

2. MODEL DEFINITION

2.1 Blades relations

Current methodologies consider only the inlet and exit rotor angles into the performance estimations, neglecting the geometric characteristics. In this paper, on the other hand, we divide the fluid passage through the rotor into 14 finite elements to enable the thermodynamic properties to be updated during the flow. To use the loss relations in each finite element, it was necessary to calculate the radius, angle β , and average cross-sectional area of each.

The Figure 1 outlines the way in which the turbine was divided.

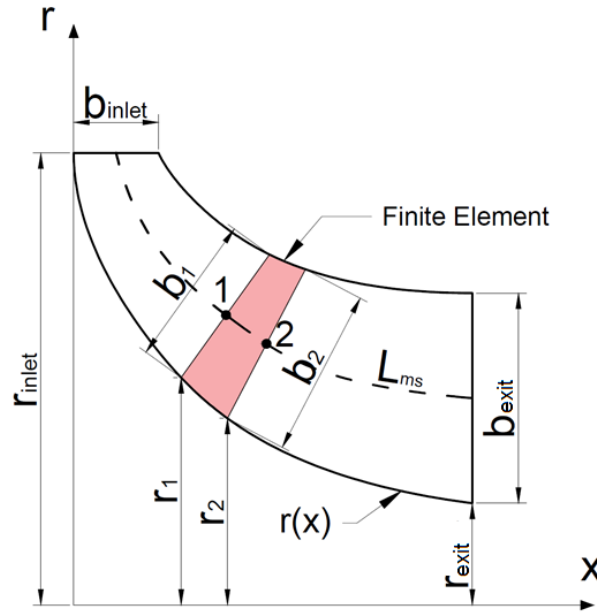


Figure 1. Function $r(x)$ and finite element

Two different geometries were tested. It was assumed that the radius varies with respect to x according to two different functions, r_1 and r_2 .

$$r_1(x) = \frac{r_{in}-r_{exit}}{n^2} x^2 - 2 \frac{r_{in}-r_{exit}}{n} x + r_{in}, \quad (1)$$

$$r_2(x) = \frac{(r_{exit}-r_{in})}{n} x + r_{in}, \quad (2)$$

where n is the number of finite elements.

The cross-sectional area, on the other hand, varies linearly from a value A_1 to a value A_2 :

$$A(x) = \frac{(A_{exit}-A_{in})}{n} x + A_{in}, \quad (3)$$

The same is true for the angle β :

$$\beta(x) = \frac{(\beta_{exit}-\beta_{in})}{n} x + \beta_{in}, \quad (4)$$

Finally, we calculate the angle alpha at the end of each finite element using the Eq. 5.

$$\alpha = \tan^{-1} \left(\frac{U_1}{C_{m2}} \frac{r_2}{r_1} - \tan \beta_2 \right), \quad (5)$$

where U_1 is the inlet Blade Linear velocity and C_{m1} is the inlet meridional velocity.

2.2 Python algorithm

To determine the performance of a turbomachinery operating with s-CO₂, a code in Python language was developed with the objective of finding the solution of the system of relations that describes the passage of the fluid through the radial turbine. To satisfy all the relations, the calculation steps followed the flowchart in “Figure 2”.

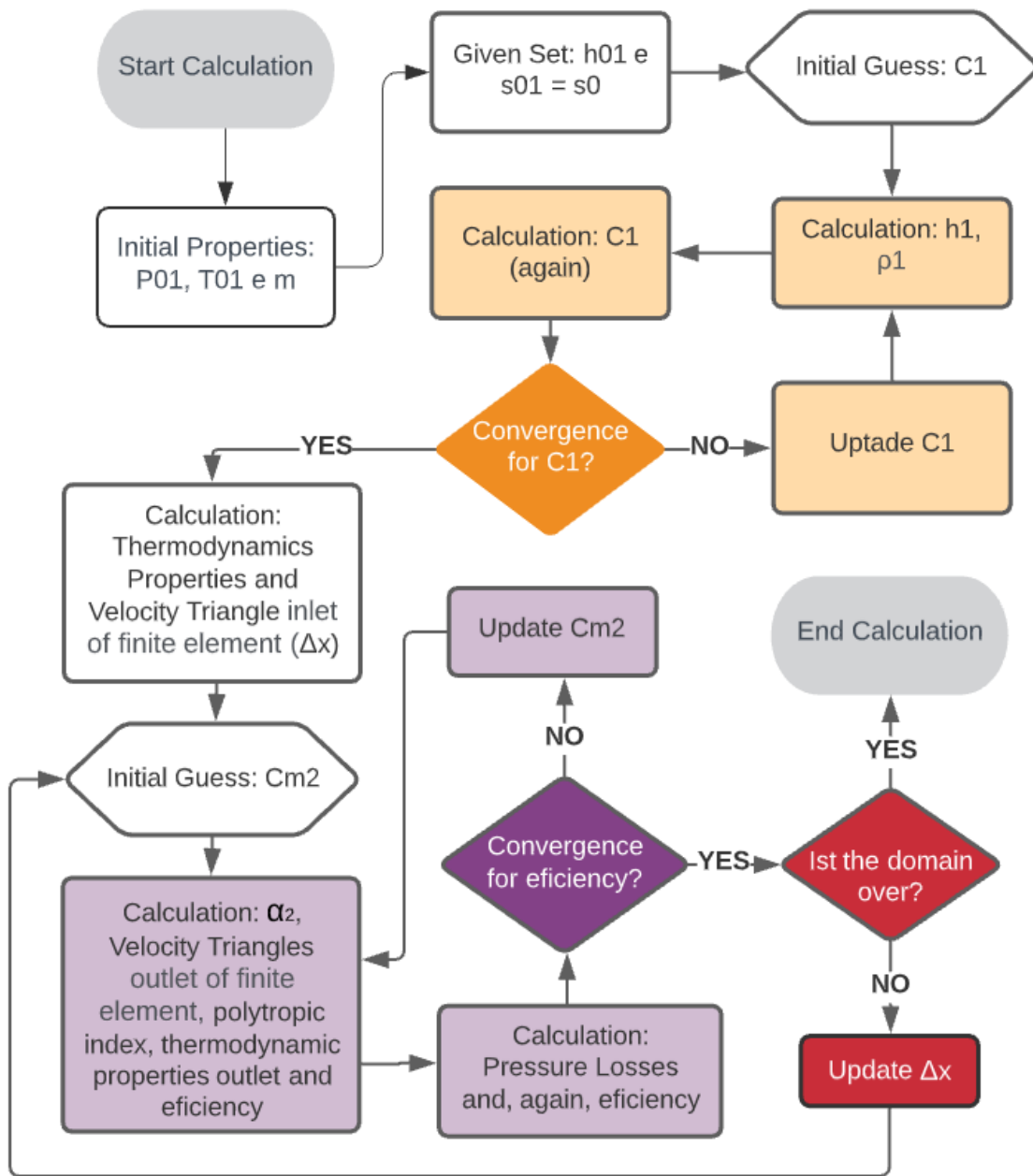


Figure 2. Schematic diagram of the Python routine

This algorithm was validated by comparing it with the results of Ventura (2012) and Lee (2020), as shown in Table 1.

Table 1. Model Validation.

	Lee (2020)	Python Algorithm	Error	Ventura (2012)	Python Algorithm	Error
Fluid	Air	Air	-	Argon	Argon	-
T₀₁	1083,3	1083,3	0,00%	1083,33	1083,33	0,00%
P₀₁	9,10E+04	9,10E+04	0,00%	9,10E+04	9,10E+04	0,00%
m	0,272	0,272	0,00%	0,2771	0,2771	0,00%
N (rpm)	38500	38176	-0,84%	38500	38502,74	0,01%
W	21400	21034,74	-1,71%	22371	22370,3	0,00%

C₁	275,7	273,38	-0,84%	uninformed	284,13	
C₂	144,84	144,84	0,00%	128,18	127,27	-0,71%
P₂	6,40E+04	64238	0,37%			
η_{ts}	0,753	0,7454	-1,01%	0,79	0,7878	-0,28%

In order to make this code possible, it was necessary to adapt the existing pressure-drop loss relations, so that they calculate the losses in each region of the turbine separately. The relations were deduced using concepts from fluid mechanics and were intended to be used for non-ideal gases. To this end, thermodynamic properties such as specific mass, specific heat, and compressibility should not be constants.

To implement a pseudo-polytropic process, the polytropic exponent from Eq. 1 had its value updated as a function of mean surface length (L_m). We used Eq. 6 to calculate the pressure and temperature at the exit of each finite element.

$$\frac{P_{02}}{P_{01}} = \left[\frac{-1 + \left(\frac{T_{02}}{T_{01}}\right)}{\eta_{ts}} + 1 \right]^{\left(\frac{n_s}{n_s - 1}\right)}, \quad (6)$$

where the indexes **01** and **02** correspond to input and output of the finite element, respectively, and n_s is the index polytropic, whose value was update in each finite element. In order to calculate n_s , equation 7 was used.

$$n_s = \frac{P_{01}}{T_{01}} \left(\frac{\partial T_{01}}{\partial P_{01}} \right)_S, \quad (7)$$

which is a partial derivative calculated at constant entropy S .

2.2 Loss Models

Six relations based on established pressure drop models for turbines was used. The pressure losses occur due to the following mechanisms: Incidence, Passage, trailing Edge, Exit Energy, Tip Clearance, and Windage. We calculated the losses to each finite element.

The Incidence loss was calculated using the relation by Whitfield and Wallace apud. Ventura (2012).

$$\Delta h_{incidence} = \frac{W_{t1}^2}{2}, \quad (8)$$

For the Passage Loss, we use the relation from Persky and Emily (2019):

$$\Delta h_{passage} = f_{curved} \frac{L}{D_H} \bar{W}^2, \quad (9)$$

where L is the length of the finite element, D_H is the hydraulic diameter and the f_{curved} is the friction factor for curved tubes, calculated from Eq. 10 by El-Genk and Schriener (2017):

$$f_{curved} = f_{straight} \cdot \left[1 + \frac{28800}{Re} \left(\frac{D_H}{D_c} \right)^{0.62} \right], \quad (10)$$

The $f_{straight}$ is the Darcy friction factor, implicitly calculated from Eq. 11:

$$\frac{1}{\sqrt{f_{straight}}} = -4 \left(\frac{\left(\frac{k_r}{D_h}\right)}{3.7} + \frac{1.256}{Re \sqrt{f_{straight}}} \right), \quad (11)$$

where k_r is the wall roughness. We used the value of 2×10^{-4} m.

Eq. 12 calculate hydraulic diameter.

$$D_h = \frac{4A}{\frac{4\pi r_1}{z_r} + \frac{AZ_r}{\pi r_1}}, \quad (12)$$

For the Trailing Edge Loss, we used Eq. 13 by Persky and Emily (2019).

$$\Delta h_{trailing} = \frac{\Delta P_{0,rel}}{\rho_{out}}, \quad (13)$$

where,

$$\Delta P_{0,rel} = P_2 \cdot \left(\frac{1+W^2}{2T_2 c_p} \right)^{\left(\frac{m}{m-1} \right)}, \quad (14)$$

The Exit Energy Loss is the Kinetic Energy of the fluid at the exit of the rotor:

$$\Delta h_{exit} = \frac{c_2^2}{2}, \quad (15)$$

For the Tip Clearance Loss, we used Eq. 16 by Persky and Sauret (2019):

$$\Delta h_{tip} = \frac{\dot{m}_{tip}}{\dot{m}} \cdot \frac{U^2}{2}, \quad (16)$$

In order to calculate \dot{m}_{tip} , we deduced an relation based on the tangential acceleration of fluid inside the rotor. It is based on the pressure difference between upstream and downstream of the blade:

$$\dot{m}_{tip} = -\frac{\bar{\rho} \omega r \varepsilon_a \varepsilon_b}{2} - \frac{\Delta P \bar{\rho} \varepsilon_b^3}{12 \bar{\mu}}, \quad (17)$$

where,

$$\Delta P = \bar{C}_m \omega (r_2 - r_1) \bar{\rho} \cos \alpha \cos \beta, \quad (18)$$

Finally, for the windage loss, the modified relation from Gosh et. al. apud Ventura (2012) was used.

$$\Delta h_{windage} = k_f \frac{\bar{\rho} \cdot U_1^3 \cdot r_1^2}{2 \cdot \dot{m} \cdot W_2^2} \cdot \frac{L}{L_H}, \quad (19)$$

where,

$$k_f = \frac{3.7 \cdot \left(\frac{\varepsilon_b}{r_1} \right)^{0.1}}{Re^{\frac{1}{2}}}, \text{ if } Re < 10^5; \frac{0.102 \cdot \left(\frac{\varepsilon_b}{r_1} \right)^{0.1}}{Re^{\frac{1}{5}}}, \text{ if } Re > 10^5, \quad (20)$$

and L_H is the length hydraulic, calculated for Eq. 21 by Ventura (2012):

$$L_H = \frac{\pi}{4} \cdot \left[\left(z_r - \frac{b_4}{2} \right) + \left(r_4 - r_{tt} - \frac{b_t}{2} \right) \right], \quad (21)$$

The total-to-static efficiency is then calculated by:

$$\eta_{ts} = \frac{\Delta h_0}{\Delta h_0 - \Delta h_{losses}}, \quad (22)$$

where,

$$\Delta h_{losses} = \Delta h_{incidence} + \Delta h_{passage} + \Delta h_{trailing} + \Delta h_{exit} + \Delta h_{tip} + \Delta h_{windage}, \quad (23)$$

3. RESULTS AND DISCUSSION

We compare the total-to-static efficiency of the polytropic and pseudo-polytropic expansion in the two turbines, one with a linear blade profile and one with a quadratic profile. The Table 1 shows the results.

Table 1. Results for performances of different turbines operating with supercritical CO₂.

Type of process	Power (W)	Efficiency
Polytropic Expansion / linear profile blade	7983	65,49%
Polytropic Expansion / quadratic profile blade	8170	69,05%
Pseudopolytropic expansion / linear profile blade	7997	65,56%
Pseudopolytropic expansion / quadratic profile blade	8182	69,09%

The polytropic coefficient varied along with the flow as shown in Figure 3.

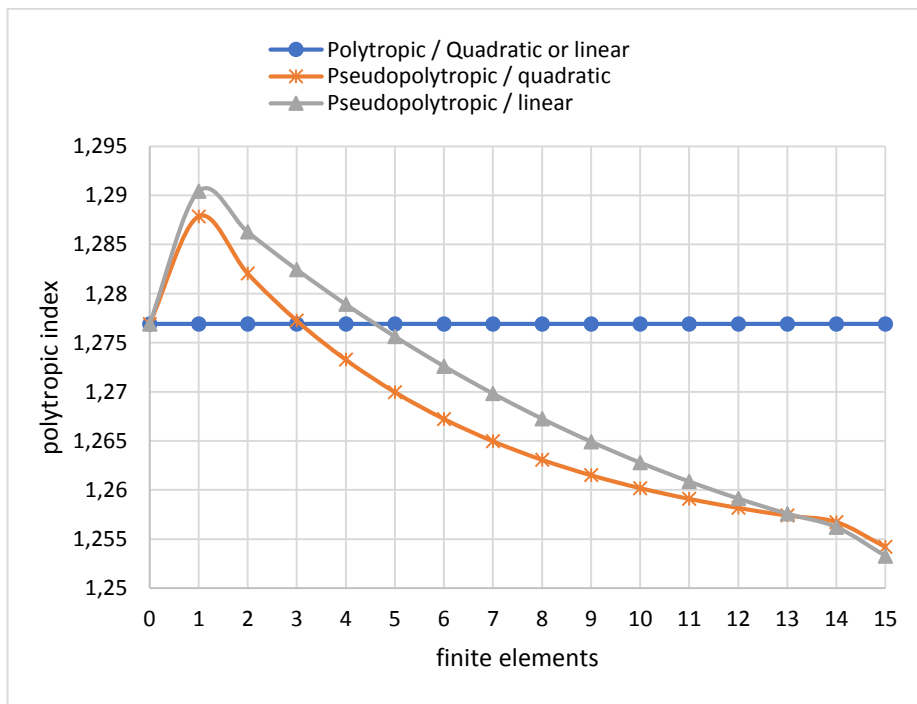


Figure 3. Polytropic index along the flow

We observe that the pseudo-polytropic expansion model results in a higher efficiency compared to the polytropic model. However, this difference is very small. In contrast, the change in blade geometry implied a difference of approximately 4 percentage points.

Figure 4 shows the evolution of enthalpy along the flow of CO₂ for an polytropic expansion. The graph for the pseudopolytropic expansion is visually the same, because the difference is not noticeable.

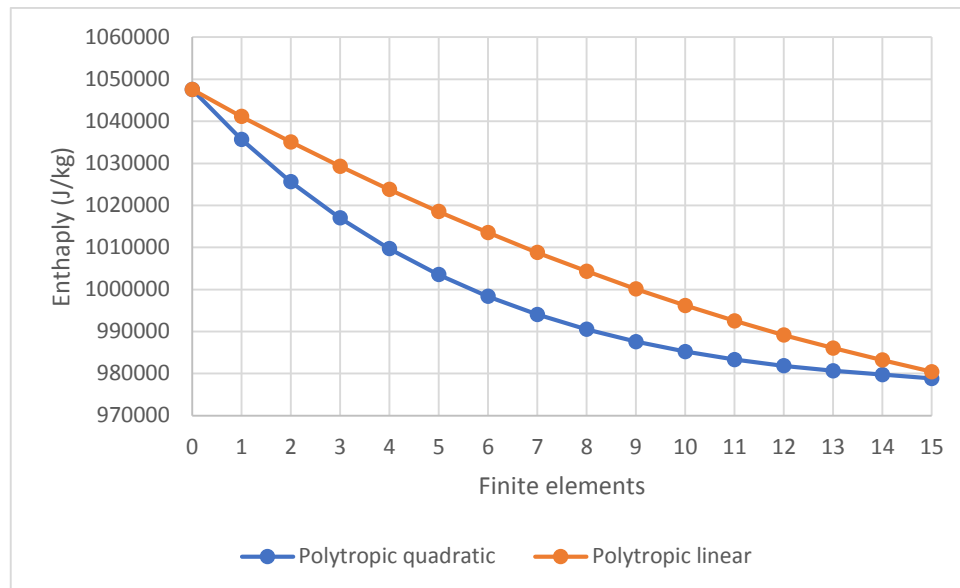


Figure 4. Enthalpy along the flow

We find that the biggest difference between the thermodynamic properties of CO₂ in both cases is in the middle region of the rotor. When the fluid reaches the region near the exit, the two curves converge, but do not touch.

If there were no pressure losses, the turbine power would depend only on the inlet and exit geometry, because the calculation could be made as a function of the variation in the momentum of fluid. Therefore, the tendency is for the curves to meet at the end. Since there are losses, the turbine power also depends on the fluid path, because different geometries produce different head losses. So even though the two curves in Fig. 2 converge, they do not meet.

3. CONCLUSION

The calculation methodology used in this paper made it possible to visualize the behavior of s-CO₂ inside the rotor. We were able to visualize the thermodynamic properties of the fluid at any point in the flow channel, using not only the relations of thermodynamics, but also three relations that describe the shape of the blade in a simplified manner.

We found that the polytropic and pseudopolytropic models resulted in close efficiency values. The difference between them was less than 1%. However, turbines with different blades have significantly different efficiencies, even if the inlet and exit of the rotor are identical. This difference could only be verified because we divided the rotor into finite elements and calculated the thermodynamic properties in each of them.

For future work, we suggest making modifications to the relations for blade geometry, in order to find the shape of the impeller that exploits the full potential of supercritical CO₂.

4. ACKNOWLEDGEMENTS

The authors thank the Federal University of Minas Gerais and FAPEMIG (Foundation for Research Support of the State of Minas Gerais)

5. REFERENCES

- BALTADJIEV N. D.; LETTIERI, C.; ZOLTÁN, S. S. An Investigation of Real Gas Effects in Supercritical CO₂ Centrifugal Compressors. Vol. 37, set 2015.
- EL-GENK M. S.; SCHRIENER, T. M. A Review and Correlations for Convection Heat Transfer and Pressure Losses in Toroidal and Helically Coiled Tubes. Heat Transfer Engineering, Vol. 38 no 5, 447-474.
- LEE, S.; GURGENCI, H. A Comparison of Three Methodological Approaches for Meanline Design of Supercritical CO₂ Radial Inflow Turbines. Energy Conversion and Management. Fev 2020.
- PERSKY, R.; SAURET, E. Loss Models for on and off-design performance of radial inflow turbomachinery. Applied Thermal Engineering. Vol. 150, Jan 2019.
- PORTO, M. P.; COIMBRA, C. F. M. On the Accuracy of Thermodynamics Numerical Simulations Using Polytropic and Pseudo-polytropic Analysis for Supercritical CO₂.

TANG, S. et. al. Optimization design for supercritical carbon dioxide compressor based on simulated annealing algorithm. *Annals of Nuclear Energy*. Vol. 140, Out 2019.

VENTURA, A. M. V. et. al. Preliminary Design and Performance Estimation of Radial Inflow Turbines Na Automated Approach. *Journal of Fluids Engineering*. Vol. 134, Mar 2012.

QI, J.; et. al. Supercritical CO₂ Radial Turbine Design Performance as a Function of Turbine Size Parameters. *Journal of Turbomachinery*. Vol. 139. Aug 2017.

6. RESPONSIBILITY NOTICE

The authors are the only responsible for the printed material included in this paper.